

Hydrido–Carbonyl Chain Clusters. Synthesis, Solid State Structure, and Solution Behavior of the Tetranuclear Open Cluster Anions $[\text{Re}_4\text{H}(\mu\text{-H})_2(\text{CO})_{17}]^-$ and $[\text{Re}_4(\mu\text{-H})(\text{CO})_{18}]^-$

Mirka Bergamo, Tiziana Beringhelli,* and Giuseppe D'Alfonso*

Dipartimento di Chimica Inorganica, Metallorganica e Analitica, Centro CNR, via Venezian 21, 20133 Milano, Italy

Pierluigi Mercandelli, Massimo Moret,* and Angelo Sironi

Dipartimento di Chimica Strutturale e Stereochimica Inorganica, via Venezian 21, 20133 Milano, Italy

Received April 18, 1997[®]

The addition of $[\text{Re}_2\text{H}(\text{CO})_9]^-$ to the electronically unsaturated complex $[\text{Re}_2(\mu\text{-H})_2(\text{CO})_8]$ rapidly and selectively gives the anion $[\text{Re}_4\text{H}(\mu\text{-H})_2(\text{CO})_{17}]^-$ (**2**), containing an open chain tetranuclear metal skeleton, as revealed by a single-crystal X-ray analysis of its $[\text{NET}_4]^+$ salt. In the solid state the three metal–metal interactions display a staggered–eclipsed–staggered conformation, while in solution ^1H and ^{13}C NMR spectra have shown conformational freedom around the three Re–Re interactions and a dynamic process exchanging the two hydrides bound to the terminal $\text{H}_2\text{Re}(\text{CO})_4$ moiety, as well as the carbonyls *trans* to them ($E_a = 48(1)$ kJ/mol). A windshield-wiper motion of the $\text{H}_2\text{Re}(\text{CO})_4$ fragment around the two *trans* diaxial carbonyls, analogous to that previously observed in the related anions $[\text{Re}_3\text{H}(\mu\text{-H})(\text{CO})_{13}]^-$ and $[\text{Re}_2\text{H}_2(\mu\text{-H})(\text{CO})_8]^-$, is likely responsible for this exchange. The tetrametallic skeleton of the anion **2** in solution easily undergoes fragmentation to trinuclear species. Under CO atmosphere the clean formation of $[\text{ReH}(\text{CO})_5]$ and $[\text{Re}_3\text{H}(\mu\text{-H})(\text{CO})_{13}]^-$ has been recognized. The anion **2** is formed (even if in lower yields) also by reaction of $[\text{Re}_2\text{H}_2(\mu\text{-H})(\text{CO})_8]^-$ with “ $\text{Re}_2(\text{CO})_9(\text{THF})$ ”, obtained by treatment of $[\text{Re}_2(\text{CO})_{10}]$ with Me_3NO in THF. A ^{13}C NMR investigation has clarified that such “ $\text{Re}_2(\text{CO})_9(\text{THF})$ ” reagent is indeed a mixture of three *eq*- $[\text{Re}_2(\text{CO})_9\text{L}]$ species, containing THF, H_2O , and, in a minor amount, NMe_3 , as labile L ligands. The reaction of the same *eq*- $[\text{Re}_2(\text{CO})_9\text{L}]$ species with $[\text{Re}_2\text{H}(\text{CO})_9]^-$ affords in good yields the tetranuclear cluster anion $[\text{Re}_4(\mu\text{-H})(\text{CO})_{18}]^-$ (**3**). The single-crystal X-ray analysis of $[\text{NET}_4]^+\mathbf{3}$ has revealed also in this case a Re_4 chain, with an all-staggered conformation, of idealized C_2 symmetry. The low-temperature ^{13}C NMR spectrum of the carbonyls has shown a higher symmetry in solution, suggesting conformational freedom around all of the Re–Re interactions.

Introduction

Tetranuclear hydrido–carbonyl clusters of rhenium exhibit a wide variety of geometries of the metal cages and of valence electron numbers (ves) (see Table 1), ranging from 56 in the “super-unsaturated” tetrahedral species $[\text{Re}_4(\mu_3\text{-H})_4(\text{CO})_{12}]^1$ to 64 in the spiked-triangle anion $[\text{Re}_4\text{H}(\mu\text{-H})_3(\text{CO})_{15}]^{2-7}$ and in the square neutral complex $[\text{Re}_4(\mu\text{-H})_4(\text{CO})_{16}]^8$. We report here the synthesis and the full characterization of two novel

clusters, which contain four rhenium atoms linked by only three metal–metal connections, a type of geometry which is unprecedented for pure hydrido–carbonyl clusters.

The novel complexes have been obtained through the two synthetic approaches (Scheme 1) that previously allowed the synthesis of the trinuclear open cluster anion $[\text{Re}_2(\text{CO})_9\{\mu\text{-H}\text{ReH}(\text{CO})_4\}]^-$,⁹ i.e., (i) the addition of a metal–carbonylate to the unsaturated dinuclear complex $[\text{Re}_2(\mu\text{-H})_2(\text{CO})_8]$ or (ii) the substitution of a labile ligand L in *eq*- $[\text{Re}_2(\text{CO})_9\text{L}]$ by an anionic rhenium hydrido complex, as detailed in the following.

Results and Discussion

The reaction of $[\text{Re}_2(\mu\text{-H})_2(\text{CO})_8]$ (**1**) with an equimolar amount of $[\text{Re}_2\text{H}(\text{CO})_9]^-$ ^{10,11} in THF at 250 K causes

[®] Abstract published in *Advance ACS Abstracts*, August 15, 1997.

(1) Saillant, R.; Barcelo, G.; Kaesz, H. *J. Am. Chem. Soc.* **1970**, *92*, 5739. Wilson, R. D.; Bau, R. *J. Am. Chem. Soc.* **1976**, *98*, 4687.

(2) Beringhelli, T.; D'Alfonso, G.; Ciani, G.; Molinari, H. *J. Chem. Soc., Chem. Commun.* **1987**, 486.

(3) Kaesz, H. D.; Fontal, B.; Bau, R.; Kirtley, S. W.; Churchill, M. R. *J. Am. Chem. Soc.* **1969**, *91*, 1021. Ciani, G.; Sironi, A.; Albano, V. G. *J. Organomet. Chem.* **1977**, *136*, 339.

(4) Beringhelli, T.; D'Alfonso, G.; Minoja, A. P.; Ciani, G.; Sironi, A. *J. Organomet. Chem.* **1992**, *440*, 175.

(5) Beringhelli, T.; Ciani, G.; D'Alfonso, G.; De Maldè, V.; Sironi, A.; Freni, M. *J. Chem. Soc., Dalton Trans.* **1986**, 1051.

(6) Bau, R.; Fontal, B.; Kaesz, H. D.; Churchill, M. R. *J. Am. Chem. Soc.* **1967**, *89*, 6374.

(7) Ciani, G.; Albano, V. G.; Immirzi, A. *J. Organomet. Chem.* **1976**, *121*, 237.

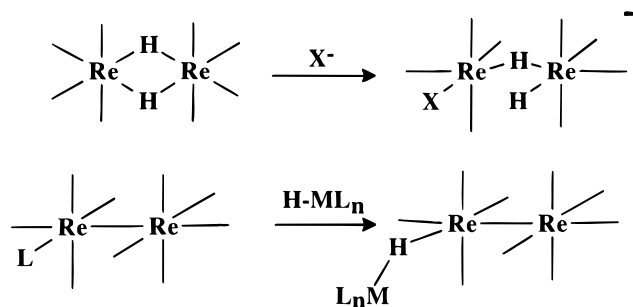
(8) Masciocchi, N.; Sironi, A.; D'Alfonso, G. *J. Am. Chem. Soc.* **1990**, *112*, 9395.

(9) Bergamo, M.; Beringhelli, T.; D'Alfonso, G.; Ciani, G.; Moret, M.; Sironi, A.; *Organometallics* **1996**, *15*, 3876.

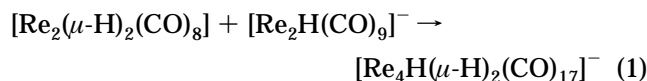
(10) Casey, C. P.; Neumann, S. M. *J. Am. Chem. Soc.* **1978**, *100*, 2544.

Table 1. Tetranuclear Hydrido–Carbonyl Clusters of Rhenium

compound	cluster geometry	ves	ref
$[\text{Re}_4(\mu_3\text{-H})_4(\text{CO})_{12}]$	tetrahedral	56	1
$[\text{Re}_4(\mu\text{-H})_3(\mu_3\text{-H})_2(\text{CO})_{12}]^-$	tetrahedral	58	2
$[\text{Re}_4(\mu\text{-H})_6(\text{CO})_{12}]^{2-}$	tetrahedral	60	3
$[\text{Re}_4(\mu\text{-H})_4(\text{CO})_{13}]^{2-}$	tetrahedral	60	4
$[\text{Re}_4(\mu\text{-H})_5(\text{CO})_{14}]^-$	butterfly	62	5
$[\text{Re}_4(\text{CO})_{16}]^{2-}$	rhomb	62	6
$[\text{Re}_4\text{H}(\mu\text{-H})_3(\text{CO})_{15}]^{2-}$	spiked-triangle	64	7
$[\text{Re}_4(\mu\text{-H})_4(\text{CO})_{16}]$	square	64	8
$[\text{Re}_4\text{H}(\mu\text{-H})_2(\text{CO})_{17}]^-$	chain	66	this work
$[\text{Re}_4(\mu\text{-H})(\text{CO})_{18}]^-$	chain	66	this work

Scheme 1

the instantaneous formation of the addition derivative $[\text{Re}_4\text{H}(\mu\text{-H})_2(\text{CO})_{17}]^-$ (**2**), according to reaction 1. The



reaction is fast and selective, as judged by IR and NMR monitoring. The formulation of the product has been established from ^1H and ^{13}C NMR characterization and by a single-crystal X-ray analysis.

Solid State Structure of $[\text{Re}_4\text{H}(\mu\text{-H})_2(\text{CO})_{17}]^-$ (**2**).

The crystal structure of **2** consists of the packing of discrete anions and cations with normal van der Waals contacts. The molecular structure of **2** is depicted in Figure 1 with a partial labeling scheme. A selection of bond parameters is reported in Table 2.

Differently from known tetranuclear hydrido–carbonyl rhenium compounds (see Table 1), anion **2** exhibits an open chain metal skeleton. Similar metal frameworks have been found previously in trinuclear rhenium clusters, namely, $[\text{Re}_3(\mu\text{-H})(\text{CO})_{14}]^{12}$ and $[\text{Re}_3\text{H}(\mu\text{-H})(\text{CO})_{13}]^-$.⁹ The formal replacement of a $\text{Re}(\text{CO})_5$ unit in $[\text{Re}_3\text{H}(\mu\text{-H})(\text{CO})_{13}]^-$ with a $\text{Re}_2(\text{CO})_9(\mu\text{-H})$ moiety to obtain **2** gives rise to a conformationally more versatile molecule, extending the L-shape of $[\text{Re}_3\text{H}(\mu\text{-H})(\text{CO})_{13}]^-$ to clusters with higher nuclearity. Anion **2** bears a total of three hydrides of which one $\mu\text{-H}$ ligand is connected to $\text{Re}(2)$, two $\mu\text{-H}$ ligands are linked to $\text{Re}(3)$, and one $\mu\text{-H}$ ligand plus the terminal hydride interact with $\text{Re}(4)$. All Re atoms attain a distorted octahedral coordination assuming as usual the $\text{M}-(\mu\text{-H})-\text{M}$ interactions as occupying a coordination site. Cluster **2** displays one short ($\text{Re}(1)-\text{Re}(2)$ 3.0641(4) Å) and two long ($\text{Re}(2)-\text{Re}(3)$ 3.4040(4) Å, $\text{Re}(3)-\text{Re}(4)$ 3.2968(3) Å) $\text{Re}-\text{Re}$ interactions, respectively depending on the absence or presence of a bridging hydride.

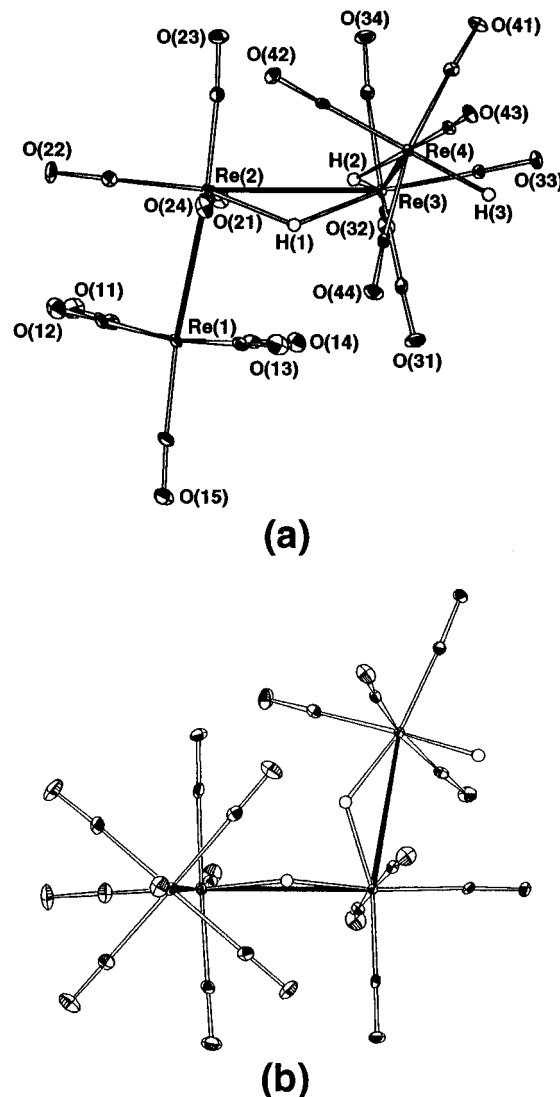


Figure 1. ORTEP views of the $[\text{Re}_4\text{H}(\mu\text{-H})_2(\text{CO})_{17}]^-$ anion **2** with partial labeling scheme: (a) along the normal to the $\text{Re}(1)/\text{Re}(2)/\text{Re}(3)$ plane; (b) after 90° rotation around the $\text{Re}(2)-\text{Re}(3)$ vector. Thermal ellipsoids are drawn at the 30% probability level. Hydride ligands were given an arbitrary small radius.

The conformation of the title anion, i.e., the relative rotation of the different ReL_x units about the $\text{Re}-\text{Re}$ vectors, deserves a detailed description. Among many different accessible conformations observed in solution (see NMR description) the one frozen and observed in the solid state seems to efficiently accommodate the intramolecular nonbonding interactions. In particular, the $\text{Re}(1)-\text{Re}(2)-\text{Re}(3)-\text{Re}(4)$ torsion ($-104.25(1)^\circ$) allows for the presence of two bridging hydride ligands on adjacent $\text{Re}-\text{Re}$ edges, both lying almost coplanar with three Re atoms (H(1) about 0.17 Å out of the $\text{Re}(1)/\text{Re}(2)/\text{Re}(3)$ plane and H(2) about 0.22 Å out of the $\text{Re}(2)/\text{Re}(3)/\text{Re}(4)$ plane). The terminal ReL_5 units appear staggered with respect to the corresponding $\text{Re}(\text{CO})_4$ fragments (see torsions in Table 2). On the contrary, the inner $\text{Re}(\text{CO})_4(\mu\text{-H})\text{Re}(\text{CO})_4$ moiety is almost eclipsed ($\text{C}(23)-\text{Re}(2)-\text{Re}(3)-\text{C}(34)$ $-16.0(3)^\circ$) with the $\text{Re}(1)(\text{CO})_5$ group facing ligand $\text{CO}(31)$ and not the bulkier $\text{Re}(4)\text{H}(\text{CO})_4$ fragment. Thus, with respect to the description of the staggering/eclipsing features of this class of clusters, **2** can be summarized as a *s/e/s*

(11) Beringhelli, T.; D'Alfonso, G.; Ghidorsi, L.; Ciani, G.; Sironi, A.; Molinari, H. *Organometallics* **1987**, *6*, 1365.

(12) (a) Fellmann, W.; Kaesz, H. D. *Inorg. Nucl. Chem. Lett.* **1966**, *2*, 63. (b) Yang, C. S.; Cheng, C. P.; Guo, L. W.; Wuang, J. *J. Chin. Chem. Soc. (Taipei)* **1985**, *32*, 17.

Table 2. Selected Bond Lengths (Å) and Angles (deg) for 2 and 3

	2	3
Re(1)–Re(2)	3.0641(4)	3.0990(9)
Re(2)–Re(3)	3.4040(4)	3.3244(11)
Re(3)–Re(4)	3.2968(3)	3.0959(11)
Re(1)–C(11)	1.994(8)	1.976(14)
Re(1)–C(12)	1.976(8)	1.981(14)
Re(1)–C(13)	1.972(8)	1.984(14)
Re(1)–C(14)	1.986(8)	1.991(13)
Re(1)–C(15)	1.948(7)	1.928(13)
Re(2)–C(21)	2.003(7)	1.979(14)
Re(2)–C(22)	1.924(8)	1.905(13)
Re(2)–C(23)	1.918(7)	1.925(12)
Re(2)–C(24)	1.994(7)	1.996(12)
Re(3)–C(31)	1.994(7)	1.980(14)
Re(3)–C(32)	1.922(7)	1.920(13)
Re(3)–C(33)	1.943(7)	1.919(12)
Re(3)–C(34)	2.010(7)	1.974(14)
Re(4)–C(41)	1.982(7)	1.987(14)
Re(4)–C(42)	1.968(7)	1.973(12)
Re(4)–C(43)	1.919(7)	1.969(13)
Re(4)–C(44)	2.001(7)	2.012(13)
Re(4)–C(45)		1.899(14)
Re(1)–Re(2)–Re(3)	101.407(10)	111.96(3)
Re(2)–Re(3)–Re(4)	99.084(9)	110.38(3)
C(11)–Re(1)–Re(2)	86.6(2)	87.6(3)
C(12)–Re(1)–Re(2)	87.1(2)	84.7(3)
C(13)–Re(1)–Re(2)	84.3(2)	84.7(3)
C(14)–Re(1)–Re(2)	81.6(2)	87.3(3)
C(15)–Re(1)–Re(2)	174.3(2)	177.4(4)
C(21)–Re(2)–Re(1)	88.7(2)	85.9(3)
C(22)–Re(2)–Re(1)	85.0(2)	81.2(3)
C(23)–Re(2)–Re(1)	172.6(2)	169.8(4)
C(24)–Re(2)–Re(1)	83.5(2)	85.7(3)
C(21)–Re(2)–Re(3)	86.0(2)	98.0(3)
C(22)–Re(2)–Re(3)	173.1(2)	164.2(3)
C(23)–Re(2)–Re(3)	84.4(2)	78.2(4)
C(24)–Re(2)–Re(3)	91.5(2)	80.8(3)
C(31)–Re(3)–Re(2)	101.5(2)	82.8(3)
C(32)–Re(3)–Re(2)	91.9(2)	78.1(3)
C(33)–Re(3)–Re(2)	168.7(2)	164.1(4)
C(34)–Re(3)–Re(2)	82.0(2)	98.1(3)
C(31)–Re(3)–Re(4)	89.1(2)	86.2(3)
C(32)–Re(3)–Re(4)	169.0(2)	171.5(3)
C(33)–Re(3)–Re(4)	77.6(2)	83.3(4)
C(34)–Re(3)–Re(4)	88.5(2)	85.1(4)
C(41)–Re(4)–Re(3)	82.8(2)	89.0(4)
C(42)–Re(4)–Re(3)	100.7(2)	85.4(4)
C(43)–Re(4)–Re(3)	164.7(2)	83.9(4)
C(44)–Re(4)–Re(3)	95.1(2)	83.8(4)
C(45)–Re(4)–Re(3)		177.7(4)
Re(1)–Re(2)–Re(3)–Re(4)	–104.25(1)	47.47(3)
C(12)–Re(1)–Re(2)–C(24)	49.5(3)	47.3(5)
C(23)–Re(2)–Re(3)–C(34)	–16.0(3)	
C(23)–Re(2)–Re(3)–C(32)		47.2(6)
C(34)–Re(3)–Re(4)–C(42)	57.4(3)	43.6(4)

conformer (*s* = staggered; *e* = eclipsed, starting from atom Re(1)). In view of the observation⁹ that Re(μ -H)-Re interactions are longer when the ligands are eclipsed, here we observe that (*e*)-Re(2)–Re(3) is elongated in comparison to (*s*)-Re(3)–Re(4), and among the longest found in hydrido–carbonyl rhenium compounds, in order to relax the steric interactions between the bulky Re(4)H(CO)₄ unit and the ligands on Re(2). The fruitful interlocking of octahedral Re centers produces effects also on the Re–Re–Re angles.⁹ In the present case, [Re₂(CO)₉(μ -H)Re(CO)₄(μ -H)ReH(CO)₄] (**2**) displays intermediate values (101.407(10) and 99.084(9)°, *s/e/s*) compared to [Re₂(CO)₉(μ -H)Re(CO)₅] (107.3°, *s/s*),¹² [Re₂(CO)₉(μ -H)ReH(CO)₄][–] (103.01(2)°, *s/s*),⁹ and [MnRe(CO)₉(μ -H)Re(CO)₅] (98.09(7)°, *s/e*).¹³

NMR Studies and Solution Behavior of 2. The ¹H NMR spectrum of **2** at 193 K displays three hydridic

resonances, one in the region of the terminal hydrides (δ –5.98) and two in the region typical of hydrides bridging Re–Re interactions (δ –16.31 and –17.13). The assignment of these resonances to H(3), H(2), and H(1), respectively, is straightforward, due to a fluxional process that interchanges the terminal and the bridging hydrides bound to Re(4), namely, H(3) and H(2) (*vide infra*).

The low-temperature ¹³C{¹H} NMR spectrum of **2** shows 11 signals in the carbonyl region, whose assignments, reported in Figure 2a, arise from the following arguments.

The resonances of the carbonyls of Re(CO)₅ moieties usually broaden when the temperature is raised, and this allows their easy identification: at 253 K (Figure 3a) the signal of B is already buried in the noise and that of the four carbonyls A is a broad hump. This broadening, already observed in the related anion [Re₃H(μ -H)(CO)₁₃][–],⁹ is likely due to the coupling with the quadrupolar isotopes of rhenium (¹⁸⁵Re natural abundance 37.07%, *I* = 5/2; ¹⁸⁷Re natural abundance 62.93%, *I* = 5/2), rather than to a dynamic process. In fact, for the high symmetry and the conformational freedom of the terminal moiety, the relaxation time of Re(1) is probably longer and more sensitive to the change of the temperature than those of the other metals. This makes the carbonyls bound to it not effectively “decoupled”.

The assignment of the lowest field resonance, of intensity 2, to carbonyls C is straightforward from the comparison of the spectra of a fully ¹³CO enriched sample (Figure 3a) and of a sample selectively enriched in the carbonyls bound to Re(3) and Re(4) (Figure 3b), obtained by reaction of natural abundance [Re₂H(CO)₉][–] with ¹³CO-enriched [Re₂(μ -H)₂(CO)₈]. This comparison also allows the identification of the resonances of D and E. The other assignments reported in Figure 2 have been made on the bases of selective ¹H decouplings, as detailed in the caption of Figure 2.

Interestingly, resolved C–H couplings are observed only for the carbonyls L and M/N coupled with the terminal hydride (*J*_{CH} = 7.3, 3.7, and 5.4 Hz, respectively) in agreement with the lower values of the coupling constants usually exhibited by bridging hydrides with respect to the terminal ones.

The conformational freedom of the whole molecule is quite high. On the basis of the solid state structure, 17 carbonyl resonances were expected, instead of the 11 observed: the equivalence, even at 193 K, of the four equatorial carbonyls A on Re(1) and of the three couples of mutually *trans* carbonyls C on Re(2), F on Re(3), and L on Re(4) implies free rotation around the Re–Re and Re(μ -H)Re bonds.

On raising the temperature, both the ¹H and the ¹³C spectra show the occurrence of dynamic processes. Above 193 K the hydridic resonances at δ –5.98 and –16.31 broaden and collapse at ca. 253 K. Also the ¹³C signals at δ 190.02 and 188.66, attributed to carbonyls M and N, *trans* to H(3) and H(2), broaden above 193 K, collapse at ca. 223 K, and eventually give rise to an averaged signal at 189.3 ppm (see Figure 3).

A similar exchange between terminal and bridging hydrides and between the related *trans* carbonyls in a

(13) (a) Kaesz, H. D.; Bau, R.; Churchill, M. R. *J. Am. Chem. Soc.* **1967**, *89*, 2775. (b) Churchill, M. R.; Bau, R. *Inorg. Chem.* **1967**, *6*, 2086.

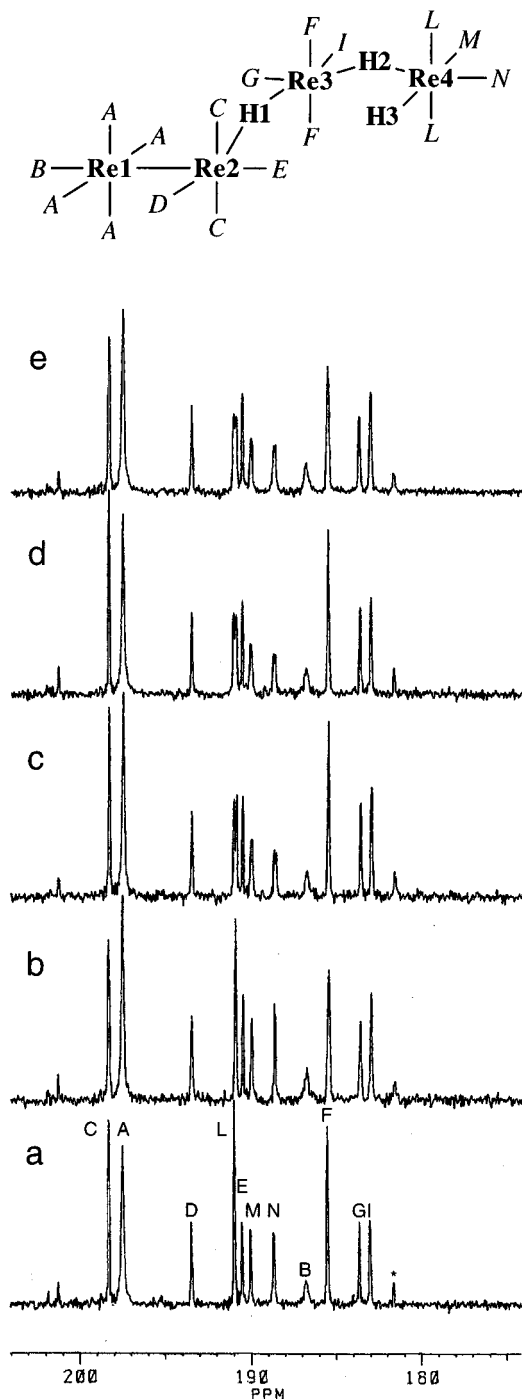


Figure 2. Carbonyl region of the ^{13}C NMR spectra of the anion **2** (193 K, 50.3 MHz, $\text{THF}-d_6$): (a) fully ^1H decoupled; (b) selectively ^1H decoupled at -5.98 ppm, H(3); (c) selectively ^1H decoupled at -16.31 ppm, H(2); (d) selectively ^1H decoupled at -17.13 ppm, H(1); (e) fully ^1H coupled. The assignment of the couples of resonances D and E, G and I, M and N can be interchanged. The comparison of spectrum e with spectrum d shows that irradiation of H(1) sharpens the resonances at 185.52 (2) and 183.66 (1) ppm (besides the signal of C) and therefore assigns the resonance of double intensity to F. The comparison of spectrum e with spectrum b shows that irradiation of H(3) decouples the signals at 190.97 (2), 190.02 (1) and 188.66 (1) ppm, assigning them to the carbonyls L, M, and N of the terminal Re(4). The asterisk marks the signal of $[\text{Re}_3(\mu\text{-H})_3(\text{CO})_{12}]$ present as an impurity in the starting material.

terminal $\text{H}_2\text{Re}(\text{CO})_4$ moiety has been observed previously in the two related anions $[\text{Re}_2\text{H}_2(\mu\text{-H})(\text{CO})_8]^-$ ¹¹

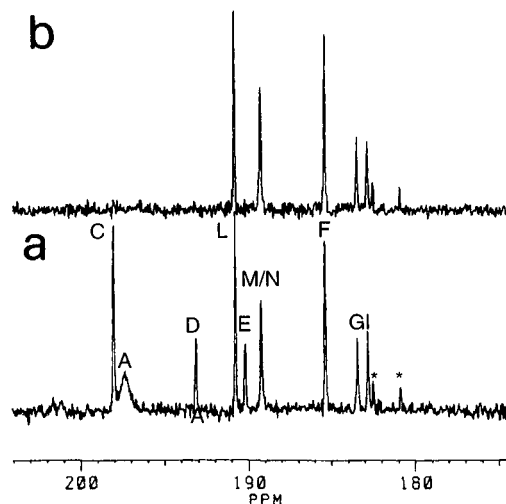
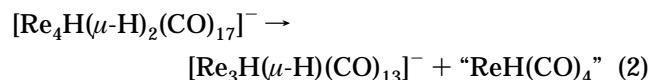


Figure 3. Carbonyl region of the ^{13}C NMR spectra of the anion **2** (253 K, 50.3 MHz, $\text{THF}-d_6$): (a) fully ^{13}C enriched; (b) selectively ^{13}C enriched in the carbonyls bound to Re(3) and Re(4). The resonance at 189.3 ppm is the signal of carbonyls M and N, averaged by fast exchange. The asterisks mark the signals of $[\text{Re}_3(\mu\text{-H})_3(\text{CO})_{12}]$ present as an impurity in the starting material.

and $[\text{Re}_3\text{H}(\mu\text{-H})(\text{CO})_{13}]^-$.⁹ This type of exchange has been attributed to a windshield-wiper motion of the terminal $\text{H}_2\text{Re}(\text{CO})_4$ moiety around the two *trans*-diaxial carbonyls. This mechanism is also likely to be operative in **2** (Scheme 2): band shape analysis performed on both the ^1H and the ^{13}C spectra indeed showed that the two processes are synchronous. The activation energy calculated accordingly is 48(1) kJ/mol. This exchange process is markedly less hindered than those observed for the homologous $[\text{Re}_3\text{H}(\mu\text{-H})(\text{CO})_{13}]^-$ ($E_a = 67(2)$ kJ/mol). For the trihydridic anion $[\text{Re}_2\text{H}_2(\mu\text{-H})(\text{CO})_8]^-$ only a ΔG^\ddagger value at the coalescence temperature is available (42 kJ/mol at 225 K), which is comparable with the value found in the present case at a similar temperature ($\Delta G^\ddagger = 44.7$ kJ/mol at 223 K).

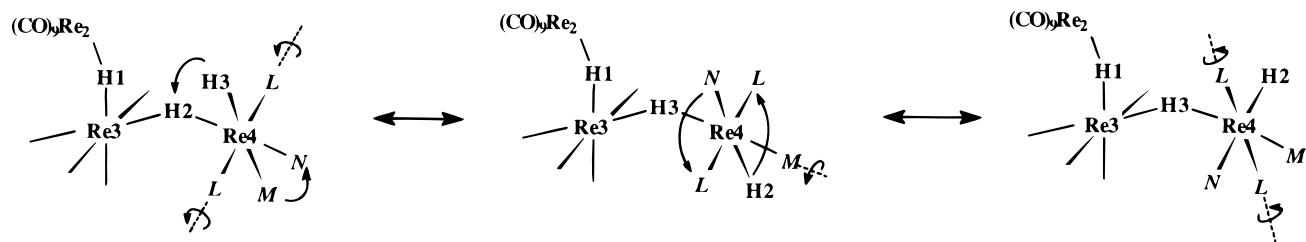
The obtention of a selective ^{13}C enrichment in the Re(3) and Re(4) sites indicates that no intramolecular CO exchange occurs in **2** (a part of the M/N interchange resulting from the fluxionality of the terminal $\text{H}_2\text{Re}(\text{CO})_4$ moiety), even in times much longer than the NMR time scale.

The stability of **2** in solution is not very high: at room temperature, in THF, the anion undergoes fragmentation, with $t_{1/2} < 4$ h, to give mixtures containing mainly the trinuclear species $[\text{Re}_3\text{H}(\mu\text{-H})(\text{CO})_{13}]^-$, $[\text{Re}_3(\mu\text{-H})_2(\text{CO})_{12}]^-$, and $[\text{Re}_3(\mu\text{-H})_3(\text{CO})_{12}]$. A possible reaction pathway accounting for this is represented by eq 2: the " $\text{ReH}(\text{CO})_4$ " fragment would be stabilized by some kind of condensation (most typically to $[\text{Re}_3(\mu\text{-H})_3(\text{CO})_{12}]$), while the open cluster $[\text{Re}_3\text{H}(\mu\text{-H})(\text{CO})_{13}]^-$ would subsequently undergo the loss of a carbonyl, to give the triangular cluster anion $[\text{Re}_3(\mu\text{-H})_2(\text{CO})_{12}]^-$, as previously reported.⁹



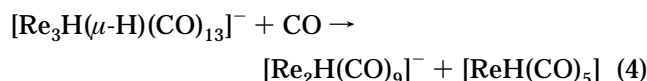
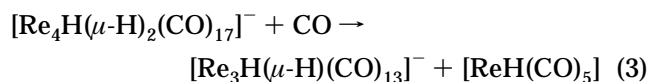
Upon treatment of **2** in refluxing THF for 24 h, the triangular $[\text{Re}_3(\mu\text{-H})_2(\text{CO})_{12}]^-$ anion is obtained as the main product. Thermal activation of **2**, therefore, does

Scheme 2

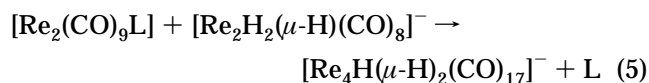


not cause decarbonylation and condensation to *closo* tetranuclear rhenium clusters, but rather results in fragmentation.

The behavior of **2** in the presence of CO is in agreement with the fragmentation represented by eq 2. The reaction has been performed at low temperature, to avoid thermal decomposition of reactants and products. NMR monitoring has shown the formation of $[\text{ReH}(\text{CO})_5]$, $[\text{Re}_3\text{H}(\mu\text{-H})(\text{CO})_{13}]^-$, and $[\text{Re}_2\text{H}(\text{CO})_9]^-$. This can be accounted for by reaction 3, followed by the previously recognized⁹ fragmentation of $[\text{Re}_3\text{H}(\mu\text{-H})(\text{CO})_{13}]^-$ (reaction 4). The integrated intensities of the resonances are in excellent agreement with this hypothesis.

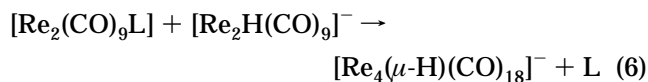


Alternative Synthesis of 2. Synthesis of $[\text{Re}_4(\mu\text{-H})(\text{CO})_{18}]^-$ (3**).** A well-established route to H-bridged polynuclear complexes involves the interaction of an H “donor” with a coordinatively unsaturated “acceptor”.¹⁴ The anion **2** can be viewed as a derivative of $[\text{Re}_2(\text{CO})_{10}]$ in which a radial carbonyl has been substituted by the $[\text{Re}_2\text{H}_2(\mu\text{-H})(\text{CO})_8]^-$ anion (acting as a ligand through a terminal Re–H bond). We therefore envisaged the preparation of **2** by reaction of $[\text{Re}_2\text{H}_2(\mu\text{-H})(\text{CO})_8]^-$ with a suitable $[\text{Re}_2(\text{CO})_9\text{L}]$ complex, containing a labile L ligand in radial position. In the previous synthesis⁹ of the L-shaped cluster anion $[\text{Re}_2(\text{CO})_9\{\text{ReH}(\mu\text{-H})(\text{CO})_4\}]^-$ good results were provided by the addition of the mononuclear anion $[\text{ReH}_2(\text{CO})_4]^-$ to the solution obtained by treating $[\text{Re}_2(\text{CO})_{10}]$ with Me_3NO , in THF. The true nature of the reactive species present in that solution will be discussed in the following. In any case, the use of this reagent provides a different route to **2**, according to eq 5.



The reaction is rather slow in THF solution (about 25% conversion after 0.5 h at room temperature), while it goes to completion in a few minutes in CH_2Cl_2 , at room temperature. However, IR and NMR monitoring show that **2** is not the only reaction product, unassignable resonances being present in the ^1H NMR spectrum in both the regions of terminal and of bridging hydrides.

Reactions such as those represented in eq 5 can in principle be carried out with any H–ML_n “ligand”, i.e., with any transition metal complex containing a terminal hydride. In line with this, we have found that the use of $[\text{Re}_2\text{H}(\text{CO})_9]^-$ easily leads to the novel tetranuclear chain cluster $[\text{Re}_4(\mu\text{-H})(\text{CO})_{18}]^-$ (**3**), according to reaction 6.

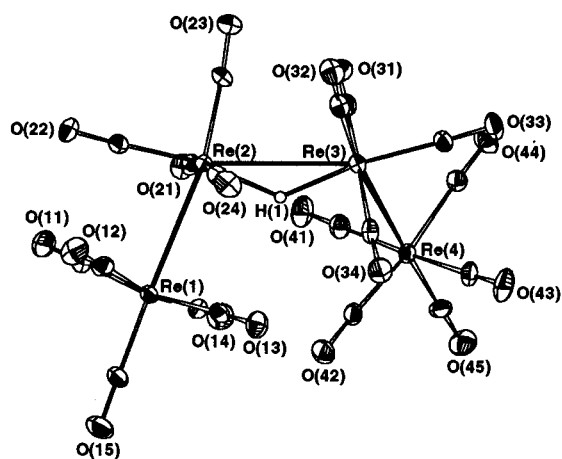


Also in this case the reaction rate is faster if a solvent different from THF is used. Differently from reaction 5, the selectivity of the reaction is quite good, on the basis of IR and NMR spectra. The anion **3** has been fully characterized by ^1H and ^{13}C NMR spectroscopy and by a solid state single-crystal X-ray diffractometric analysis.

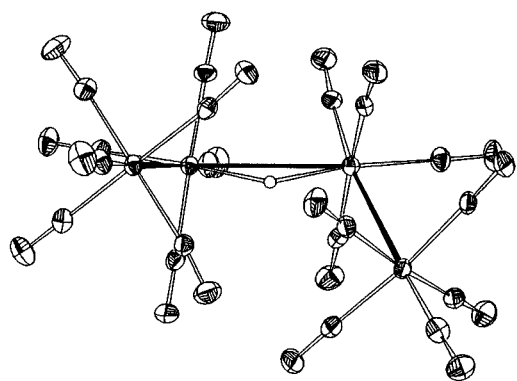
Solid State and Solution Structure of $[\text{Re}_4(\mu\text{-H})(\text{CO})_{18}]^-$ (3**).** The crystal structure of **3** consists of the packing of discrete anions and cations with normal van der Waals contacts. The molecular structure of **3** is depicted in Figure 4 with a partial labeling scheme. A selection of bond parameters is reported in Table 2.

Anion **3** shares with **2** the number of valence electrons (66) and the open chain metal skeleton. It can formally be derived by replacing an axial CO ligand of the $(\mu\text{-H})\text{Re}(\text{CO})_5$ moiety in $[\text{Re}_3(\mu\text{-H})(\text{CO})_{14}]^{12}$ with a $\text{Re}(\text{CO})_5$ group. $[\text{Re}_4(\mu\text{-H})(\text{CO})_{18}]^-$ possesses an idealized C_2 symmetry with the 2-fold axis passing through the middle point of the Re(2)–Re(3) vector and the hydride. The unique hydride ligand bridges the central Re(2)–Re(3) interaction and lies at about half distance from the Re(1)/Re(2)/Re(3) and Re(2)/Re(3)/Re(4) planes (H about 0.34 and 0.32 Å from these planes, respectively). All Re atoms attain a distorted octahedral coordination assuming the M–(μ-H)–M interaction as occupying a coordination site. Cluster **3** exhibits two short (Re(1)–Re(2) 3.0990(9) Å and Re(3)–Re(4) 3.0959(11) Å) and one long (Re(2)–Re(3) 3.3244(11) Å) Re–Re interactions, the longer one being associated with the bridging hydride. With reference to Table 2, the C–Re–Re–C torsion angles reveal an all-staggered conformation for this anion, i.e., with the previous nomenclature scheme a *s/s/s* conformation. Accordingly the Re(2)(μ-H)–Re(3) interaction in **3** is shorter than the corresponding one in **2**. The staggering of all ReL_x groups in **3** is expected to drive the 1,3⁹ and especially the 1,4 $\text{Re}\cdots\text{Re}$ interactions toward large values of the Re–Re–Re angles, in order to alleviate the eclipsing of CO ligands of facing Re centers (for a tetranuclear chain the head and tail $\text{Re}(\text{CO})_x$ groups come in close contact whenever the absolute value of the Re–Re–Re torsion angle falls near 45° or less, the 1,4 $\text{Re}\cdots\text{Re}$ distance becoming shorter as this torsion moves toward

(14) See, for instance: (a) Venanzi, L. M. *Coord. Chem. Rev.* **1982**, *43*, 251. (b) Crabtree, R. H. *Angew. Chem., Int. Ed. Engl.* **1993**, *32*, 789. (c) Bergamo, M.; Beringhelli, T.; D'Alfonso, G.; Moret, M.; Sironi, A. *Inorg. Chim. Acta* **1997**, *259*, 291.



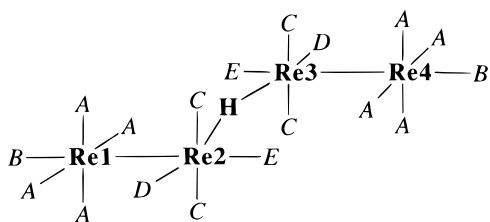
(a)



(b)

Figure 4. ORTEP views of the $[\text{Re}_4(\mu\text{-H})(\text{CO})_{18}]^-$ anion **3** with partial labeling scheme: (a) along the normal to the $\text{Re}(1)/\text{Re}(2)/\text{Re}(3)$ plane; (b) after 90° rotation around the $\text{Re}(2)\text{-Re}(3)$ vector. Thermal ellipsoids are drawn at the 30% probability level. The hydride ligand was given an arbitrary small radius.

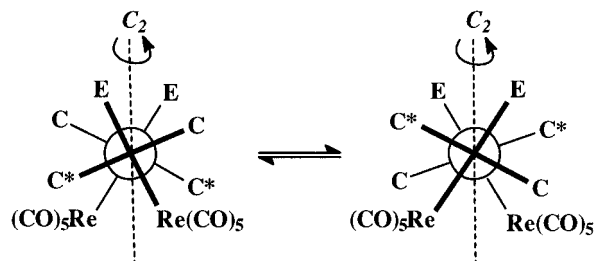
Scheme 3



zero). In **3** the $\text{Re}\text{-Re}\text{-Re}$ angles behave coherently with this picture, being the largest among related clusters ($\text{Re}(1)\text{-Re}(2)\text{-Re}(3)$ $111.96(3)^\circ$ and $\text{Re}(2)\text{-Re}(3)\text{-Re}(4)$ $110.38(3)^\circ$, to be compared with the values above reported). Therefore, even significant differences in the bond parameters within this class of compounds can be ascribed to the global optimization of the intramolecular interlocking of the $\text{Re}(\text{CO})_x$ groups.

In solution, the hydridic resonance of the anion **3** is at δ values (-17.40 ppm) typical of $\text{Re}\text{-H}\text{-Re}$ groups. The ^{13}C NMR spectrum at 193 K displays four carbonyl resonances, in the ratio 6:1:1:1. The signal of higher intensity results from the accidental overlap of the resonance due to the eight carbonyls A on $\text{Re}(1)$ and $\text{Re}(4)$ with that due to the four carbonyls C on $\text{Re}(2)$ and $\text{Re}(3)$ (see Scheme 3). This overlap is clearly recognizable at higher temperatures, where the reso-

Scheme 4

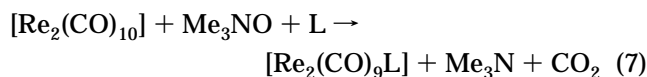


nances of carbonyls A and B of the $\text{Re}(\text{CO})_5$ moieties broaden, and almost disappear in the noise, while the resonances of carbonyls C remain sharp.

As for the anion **2**, the solution NMR spectra of **3** indicate a symmetry higher than in the solid state. The C_2 axis passing through the $\text{Re}(2)\text{-H}\text{-Re}(3)$ bond found in the idealized solid state structure would equalize $\text{Re}(1)$ with $\text{Re}(4)$ and $\text{Re}(2)$ with $\text{Re}(3)$, but could not account for the equivalence of the *trans*-diaxial carbonyls C on $\text{Re}(2)$ [and on $\text{Re}(3)$] and of the equatorial carbonyls A on $\text{Re}(1)$ [and on $\text{Re}(4)$]. Conformational freedom around the two terminal $\text{Re}\text{-Re}$ bonds and at least a libration around the central $\text{Re}\text{-H}\text{-Re}$ interaction are required to give rise to the apparent symmetry of the anion in solution (see Scheme 4). However, due to the short nonbonding interactions between the coordination spheres of $\text{Re}(1)$ and $\text{Re}(3)$ or $\text{Re}(4)$, opposing $\text{Re}\text{-Re}\text{-Re}\text{-Re}$ torsion angles below 45° , the libration around the $\text{Re}\text{-H}\text{-Re}$ bond should involve remarkable opening of the $\text{Re}\text{-Re}\text{-Re}$ angles or should occur through a -270° variation of the torsion angle.

The chain cluster anion **3** in solution is more robust than **2**, but it too slowly decomposes ($t_{1/2} > 24$ h in THF at room temperature), to unidentified nonhydridic derivatives. NMR monitoring has shown the intermediate formation of a species responsible for a hydridic resonance at $\delta -16.1$ ppm, observed also under CO. The presence of CO, indeed, did not cause any clear reaction.

The True Nature of the “ $\text{Re}_2(\text{CO})_9(\text{THF})$ ” Reagent. Decarbonylation of $[\text{Re}_2(\text{CO})_{10}]$ by Me_3NO (eq 7) represents a well-known route to substitution derivatives of $[\text{Re}_2(\text{CO})_{10}]$.¹⁵ When reaction 7 is performed in THF in the absence of added L ligands, the product(s) of the reaction provide(s) a quite useful reagent for the synthesis of open chain clusters. We have used this reagent here for the synthesis of the anions **2** and **3** (eqs 5 and 6) and in a previous work⁹ for the synthesis of the L-shaped trinuclear anion $[\text{Re}_2(\text{CO})_9(\mu\text{-H})\text{ReH}(\text{CO})_4]^-$. In ref 9 we formulated this reagent as $[\text{Re}_2(\text{CO})_9(\text{THF})]$, even if there was some evidence that more than one product was present in the reaction mixture.



A species with an identical IR spectrum in the $\nu(\text{CO})$ region and the same bright yellow color was previously obtained by Gard and Brown¹⁶ by photolysis of $[\text{Re}_2(\text{CO})_{10}]$ in THF solution. They formulated this product as $[\text{Re}_2(\text{CO})_9(\text{H}_2\text{O})]$, because of the presence of a resonance at δ ca. 6 ppm in the ^1H NMR spectrum, with the correct intensity. They used this reagent to prepare

(15) Koelle, U. *J. Organomet. Chem.* **1978**, *155*, 53

(16) Gard, D. R.; Brown, T. L. *J. Am. Chem. Soc.* **1982**, *104*, 6340.

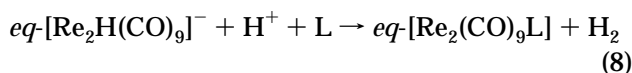
Table 3. ^{13}C NMR Data of the $\text{Re}_2(\text{CO})_9\text{L}$ Species **4** (THF- d_6 , 193 K)

4a	4b	4c	intensity	attribution
209.3	207.7	210.2	2	C
196.7	197.6	197.5	4	A
194.6	194.5	194.1	1	D/E
189.9	189.1	192.8	1	E/D
186.6	187.5	186.0	1	B

a series of substitution derivatives of $[\text{Re}_2(\text{CO})_{10}]$, including $[\text{Re}_3(\mu\text{-H})(\text{CO})_{14}]$, obtained by reaction with $[\text{ReH}(\text{CO})_5]$. They also performed the reaction of $[\text{Re}_2(\text{CO})_{10}]$ with $\text{Me}_3\text{NO}\cdot 2\text{H}_2\text{O}$, in wet THF (3% H_2O by volume), and the products were tentatively formulated as a mixture of aquo and trimethylamine complexes.

To get more insight into the nature of “ $\text{Re}_2(\text{CO})_9$ -(THF)”, a ^{13}C NMR investigation was undertaken. Samples of $[\text{Re}_2(\text{CO})_{10}]$ have been treated with anhydrous Me_3NO , in freshly anhydriated THF solution, and then evaporated to dryness and dissolved in THF- d_6 , in NMR tubes. The ^{13}C NMR spectra showed the formation of mixtures containing three species **4a**, **4b**, **4c**, in different ratios in the different experiments, **4c** being usually the minor species (10–20%). Every product exhibited five resonances (Table 3), with the 2:4:1:1:1 pattern already observed^{9,10} in $eq\text{-}[\text{Re}_2\text{H}(\text{CO})_9]^-$. Compounds **4** can therefore be formulated as $eq\text{-}[\text{Re}_2(\text{CO})_9\text{L}]$ derivatives, containing different L ligands. The solvent THF, water (unavoidable traces), the reagent Me_3NO , and the product Me_3N are the potential L ligands present in the reaction conditions.

To clarify this point, we have exploited a different route to $eq\text{-}[\text{Re}_2(\text{CO})_9\text{L}]$ complexes, involving hydride abstraction from the dinuclear anion $eq\text{-}[\text{Re}_2\text{H}(\text{CO})_9]^-$. The treatment of this complex with etherated HBF_4 , in THF at room temperature, gave bright yellow solutions with the same $\nu(\text{CO})$ IR bands observed in the mixtures from reaction 7. H_2 evolution was also revealed by GLC, confirming the occurrence of reaction 8.



^{13}C NMR analyses showed that in these conditions only two of the above species **4** were formed, namely, **4a** and **4b**, with the first one largely dominant. The solvent THF and the traces of water are the only ligands present in both reactions 7 and 8. The addition of water (6 μL , ca. 3 equiv) to the above mixture resulted in the quantitative conversion of **4a** into **4b**. At the same time, the resonance at δ 5.75, present in the ^1H NMR spectrum of the reaction mixture and attributable to coordinated water,¹⁶ acquired a higher intensity (and shifted to δ 6.11, due to increased H-bond interactions). We can therefore formulate the species **4b** as the $[\text{Re}_2(\text{CO})_9(\text{H}_2\text{O})]$ derivative previously identified by Gard and Brown,¹⁶ and the species **4a** as the true $[\text{Re}_2(\text{CO})_9\text{-}(\text{THF})]$ derivative.¹⁷ To identify **4c**, gaseous NMe_3 was distilled into an NMR tube containing a mixture of the three species **4a**, **4b**, **4c**. ^{13}C NMR monitoring at 193

(17) The resonances of coordinated THF cannot be observed in the ^1H NMR spectra, because the coordinated ligand is deuterated (the spectra are in THF- d_6 solution). The ^{13}C NMR spectra of natural abundance samples show a broad resonance at 82.2, with an intensity comparable to that due to carbonyls A, attributable to the α carbons (the resonance of the β carbons, which are expected to have a lower coordination shift, likely overlaps with the quintet of the free solvent).

K showed the increase of the resonances of **4c**, at first at the expense of **4a**, and then, at longer times, also of **4b**. In the meanwhile, the ^1H NMR spectrum showed the progressive increase of a resonance at δ 3.10, attributable to coordinated NMe_3 . The addition of an excess of Me_3NO to a mixture of **4a**, **4b**, and **4c** did not cause an increase of the signals of any of these species, but rather resulted in the appearance of novel resonances, thus confirming that the amine oxide is not a ligand present in the above species **4**.

Finally, the hypothesis that one of the species **4** contained an OH^- ligand (possibly originated by deprotonation of coordinated water in the presence of NMe_3) has been ruled out by conductivity measurements. The mixture obtained by treating $[\text{Re}_2(\text{CO})_{10}]$ with Me_3NO , in THF, had a very low conductivity (about $1.5 \mu\text{S cm}^{-1}$), that increased only slightly upon addition of water and NMe_3 (up to ca. $2.1 \mu\text{S cm}^{-1}$).

Conclusions. Carbonyl complexes containing an open array of four metal atoms were previously known,¹⁸ but the stability of these tetrametallic chains was always ensured by the presence of elements of groups 14–17 bridging the metal–metal interactions.¹⁹ To the best of our knowledge, the $[\text{Re}_4\text{H}_{2n+1}(\text{CO})_{18-n}]^-$ anions here reported ($n = 0, 1$) provide the first examples of clusters of four metal atoms linked only by three M–M or M–H–M interactions.²⁰

The great flexibility of **2** and **3** together with the high number of conformational degrees of freedom (i.e., bonds around which there can be free rotation, promoted by thermal activation in solution and by intramolecular and packing forces in the solid state) produces a complex

(18) See, for instance, the following examples, retrieved from the Cambridge Structural Data Base (release October 1996). (a) BADGIW: Braunstein, P.; Matt, D.; Fischer, J.; Mitschler, A. *J. Organomet. Chem.* **1981**, *213*, 79. (b) CAPCEB: Holand, S.; Mathey, F.; Fischer, J.; Mitschler, A. *Organometallics* **1983**, *2*, 1234. (c) COFERI10: Haines, R. J.; Steen, N. D. C. T.; English, R. B. *J. Chem. Soc., Dalton Trans.* **1983**, 1607. (d) DEHNUZ: Brauer, D. J.; Hasselkuss, G.; Hietkamp, S.; Sommer, H.; Stelzer, O. *Z. Naturforsch., Teil B* **1985**, *40*, 961. (e) DEXBIR, DEXBOX: Keijsper, J.; Polm, L. H.; van Koten, G.; Vrieze, K.; Nielsen, E.; Stam, C. H. *Organometallics* **1985**, *4*, 2006. (f) DEXBOX10: Polm, L. H.; Mul, W. P.; Elsevier, C. J.; Vrieze, K.; Christophersen, M. J. N.; Stam, C. H. *Organometallics* **1988**, *7*, 423. (g) FIJPIX, FIJPIY: Shulman, P. M.; Burkhardt, E. D.; Lundquist, E. G.; Pilato, R. S.; Geoffroy, G. L.; Rheingold, A. L. *Organometallics* **1987**, *6*, 101. (h) FOSJIG: Field, J. S.; Haines, R. J.; Honrath, U.; Smit, D. N. *J. Organomet. Chem.* **1987**, *329*, C25. (i) GALXAS: Ciriano, M. A.; Sebastian, S.; Oro, L. A.; Tiripicchio, A.; Tiripicchio Camellini, M.; Lahoz, F. J. *Angew. Chem., Int. Ed. Engl.* **1988**, *27*, 402. (j) HEDZUL: Brunet, L.; Mercier, F.; Ricard, L.; Mathey, F. *Angew. Chem., Int. Ed. Engl.* **1994**, *33*, 742. (k) JIWDAL: Lang, H.; Leise, M.; Zsolnai, L. *J. Organomet. Chem.* **1991**, *410*, 379. (l) KEJKAL; Li, P.; Curtis, M. D. *Inorg. Chem.* **1990**, *29*, 1242. (m) LEPDAL: Bruce, M. I.; Hinchliffe, J. R.; Surynt, R.; Skelton, B. W.; White, A. H. *J. Organomet. Chem.* **1994**, *469*, 89. (n) SIZPEW: Mul, W. P.; Elsevier, C. J.; van Leijen, M.; Vrieze, K.; Spek, A. L. *Organometallics* **1991**, *10*, 533. (o) TM-NORH: Böbling, D. A.; Gill, T. P.; Mann, K. R. *Inorg. Chem.* **1981**, *20*, 194. (p) VUNBOV: Akita, M.; Sugimoto, S.; Tanaka, M.; Morooka, Y. *J. Am. Chem. Soc.* **1992**, *114*, 7581. (q) VURPAZ: Braunstein, P.; Knorr, M.; Tiripicchio, A.; Tiripicchio Camellini, M. *Inorg. Chem.* **1992**, *31*, 3685. (r) WAXYID: Beers, O. C. P.; Elsevier, C. J.; Smeets, W. J. J.; Spek, A. L. *Organometallics* **1993**, *12*, 3199. (s) YORXIM: Rybin, L. V.; Osintseva, S. V.; Batsanov, A. S.; Struchkov, Yu. T.; Petrovskii, P. V.; Rybinskaya, M. I. *Izv. Akad. Nauk SSSR, Ser. Khim.* **1993**, 1285.

(19) The linear arrangement of four Rh atoms in the complex $[\text{Rh}_4(\text{s-pqdi})_2(\text{pqdi})(\text{CO})_4]^{2+}$ (pqdi = 9,10-phenanthroquinonediimine; s-pqdi = 9,10-phenanthrosemiquinonediimine) is indeed stabilized by layered δ -type bonds among π orbitals of the eclipsed ligands; Chern, S.-S.; Lee, G.-H.; Peng, S.-M. *J. Chem. Soc., Chem. Commun.* **1994**, 1645. Anyway, this complex is clearly more akin to the well-known “stacked” columnar complexes typified by $[\text{Pt}(\text{CN})_4]^{2-}$ than to a carbonyl cluster.

(20) A $[\text{Os}_4\text{H}_2(\text{CO})_{16}]$ complex has been reported as a trace byproduct of the carbonylation of OsO_4 in the presence of hydrogen, but it has never been isolated and fully characterized; Moss, J. R.; Graham, W. A. *G. Inorg. Chem.* **1977**, *16*, 75.

behavior similar to that of *n*-alkanes. In this context, it would be worthwhile examining the solid state structures of salts of the same cluster anions with different counterions. Major stereochemical differences within this class of open chain metal clusters are also expected to arise both from the nuclearity and from the number (and relative positions) of bridging hydride ligands along the chain. The possibility of further extending the scope of the methods outlined in Scheme 1 to hydrido-carbonyl complexes of higher nuclearity or containing a different number of hydrides is under current investigation in our laboratory.

Experimental Section

The reactions were performed under nitrogen, using the Schlenk technique, and solvents were deoxygenated and dried by standard methods. Literature methods were used for the preparation of $[\text{Re}_2(\mu\text{-H})_2(\text{CO})_8]^{21}$, $(\text{NEt}_4)[\text{Re}_2\text{H}(\text{CO})_9]^{11}$ and ^{13}C -enriched (about 25%) $[\text{Re}_2(\text{CO})_{10}]^{22}$. Infrared spectra were recorded on a Perkin-Elmer 781 grating spectrophotometer in a 0.1 mm CaF_2 cell. NMR spectra were recorded on Bruker AC200, Bruker WP80, and Varian Gemini 200 spectrometers. The calibration of the temperature was checked using the standard $\text{CD}_3\text{OD}/\text{CH}_3\text{OH}$ solution and controlled by BVT-1000 (Bruker) or Stelar VTC90 (Varian) units. The NMR monitoring of the reactions involving **2** was performed always at low temperature, because of the coalescence of the hydridic resonances at room temperature. ^{13}C and ^1H NMR spectra have been simulated allowing for the changes of the chemical shifts with the temperature and using an authors' modified version of the QCPE program Multi Site EXchange.²³ The goodness of the fit has been estimated visually through the superposition on the PC monitor of the simulated and experimental spectra.

Synthesis of $[\text{NEt}_4][\text{Re}_4\text{H}(\mu\text{-H})_2(\text{CO})_{17}]$ ($[\text{NEt}_4]\mathbf{2}$). A sample of $[\text{Re}_2(\mu\text{-H})_2(\text{CO})_8]$ (50 mg, 0.084 mmol) was added to a solution of $[\text{NEt}_4][\text{Re}_2\text{H}(\text{CO})_9]$ (63 mg, 0.084 mmol) in THF, at 253 K. The solution was allowed to warm up to room temperature, concentrated, and then treated with *n*-hexane, to give a pale yellow precipitate of $[\text{NEt}_4][\text{Re}_4\text{H}(\mu\text{-H})_2(\text{CO})_{17}]$ (88 mg, 0.064 mmol, isolated yield 77%). Crystals suitable for X-ray analysis were obtained from THF/*n*-hexane. Spectroscopic data of the anion **2**: IR (THF) $\nu(\text{CO})$ 2091 w, 2071 w, 2038 ms, 2003 vs, 1980 s, br, 1931 ms, 1914 m; ^1H NMR (THF- d_6 , 193 K) δ -5.98 (1), -16.31 (1), -17.13 (1).

Preparation of ^{13}C -Enriched $[\text{NEt}_4][\text{Re}_4\text{H}(\mu\text{-H})_2(\text{CO})_{17}]$, $[\text{NEt}_4]\mathbf{2}$. (a) **Fully Enriched Sample.** The reaction was performed as above, using $[\text{Re}_2(\mu\text{-H})_2(\text{CO})_8]$ and $[\text{NEt}_4][\text{Re}_2\text{H}(\text{CO})_9]$ both prepared from the same sample of ^{13}C -enriched $[\text{Re}_2(\text{CO})_{10}]$ (ca. 25%). ^{13}C NMR (THF- d_6 , 193 K): δ 198.39 (2), 197.57 (4), 193.50 (1), 190.97 (2), 190.53 (1), 190.02 (1), 188.66 (1), 186.78 (1), 185.52 (2), 183.66 (1), 183.04 (1) ppm.

(b) **Selectively Enriched Sample.** The reaction was performed in an NMR tube from natural abundance $[\text{NEt}_4][\text{Re}_2\text{H}(\text{CO})_9]$ (36 mg, 0.048 mmol) and ^{13}C -enriched $[\text{Re}_2(\mu\text{-H})_2(\text{CO})_8]$ (29 mg, 0.048) in THF- d_6 at 253 K. The ^{13}C NMR spectrum is shown in Figure 3b (THF- d_6 , 253 K): δ 190.84 (2), 189.28 (2), 185.42 (2), 183.51 (1), 182.88 (1) ppm.

Preparation of $[\text{Re}_2(\text{CO})_9(\text{L})]$. (a) **By Protonation of $[\text{Re}_2\text{H}(\text{CO})_9]^-$.** A sample of $[\text{NEt}_4][\text{Re}_2\text{H}(\text{CO})_9]$ (75 mg, 0.099 mmol) was dissolved in THF- d_6 and treated with a diethyl ether solution of HBF_4 (54%, 13.5 μL , 0.098 mmol) at 295 K. A ^{13}C NMR spectrum at 193 K showed the quantitative transformation of the hydride into the species **4a** and **4b**, with $[\text{Re}_2(\text{CO})_9(\text{THF})]$ (**4a**) largely dominant (**4a/4b** ca. 8/1). The

addition, at 293 K, of H_2O (6 μL , 0.33 mmol) gave the species **4b**. A ^1H NMR spectrum at 298 K showed the resonance of coordinated H_2O at δ 6.11 and the signal of free H_2O at δ 3.5. The reaction was repeated in the same conditions by using ^{13}C -enriched $[\text{NEt}_4][\text{Re}_2\text{H}(\text{CO})_9]$ (44 mg, 0.058 mmol) and a diethyl ether solution of HBF_4 (54%, 8 μL , 0.058 mmol) to give $[\text{Re}_2(\text{CO})_9(\text{THF})]$ (**4a**) contaminated by a very low amount of **4b**. The sample was treated at low temperature with aqueous NMe_3 (45%, 17 μL , 0.11 mmol). No immediate reaction was observed. After 3 days at 253 K, a ^{13}C NMR spectrum (193 K) showed the quantitative formation of **4b**, while a ^1H NMR spectrum (193 K) showed the resonance of coordinated H_2O at δ 6.56 and the signal of free H_2O at δ 4.35.

(b) **From $[\text{Re}_2(\text{CO})_{10}]$ and Me_3NO .** Typically, a sample of $[\text{Re}_2(\text{CO})_{10}]$ (120 mg, 0.18 mmol) was dissolved in THF at room temperature and treated with anhydrous Me_3NO (ca. 18 mg, 0.24 mmol). The solution became immediately bright yellow, and IR monitoring (1 h) showed the formation of a species with a $\nu(\text{CO})$ pattern typical of $[\text{Re}_2(\text{CO})_9(\text{L})]$ species: 2103 vw, 2041 m, 1990 vs, 1956 m, 1915 m cm^{-1} .⁹ The solvent was removed under vacuum to give an oily residue, which was dissolved in THF- d_6 ; ^{13}C -NMR spectra recorded at 193 K showed the presence of three species **4a**, **4b**, **4c** (Table 3), in variable ratios (30–70% **4a**, 60–10% **4b**, 10–20% **4c**). The same reaction was repeated with ^{13}C -enriched $[\text{Re}_2(\text{CO})_{10}]$ (40 mg, 0.061 mmol) and anhydrous Me_3NO (ca. 5 mg, 0.07 mmol). The residue was dissolved in THF- d_6 and the solution transferred into an NMR tube, analyzed, and then treated with anhydrous Me_3N , distilled directly into the tube (0.1 mL ca. at 193 K). ^{13}C NMR spectra, acquired at 193 K, showed the instantaneous conversion of **4a** into **4c** and then the slow conversion of **4b** into **4c**: before amine addition, **4a** 28%, **4b** 62%, **4c** 10%; after 0.5 h at room temperature, **4b** 62%, **4c** 38%; after 11 h, **4b** 35%, **4c** 65%. In the meanwhile the ^1H NMR spectra (193 K) showed the broadening and the low-field shift (and eventually the decrease) of the resonance due to water coordinated in **4b** (from δ 6.31 to 8.26 ppm), accompanied by the increase of the intensity of resonances due to free water (δ 4.47) and coordinated Me_3N (δ 3.09) (free Me_3N being at δ 2.1 ppm). The same reaction was repeated *in situ* in a NMR tube by treating ^{13}C -enriched $[\text{Re}_2(\text{CO})_{10}]$ (36 mg, 0.055 mmol) with 2 equiv of anhydrous Me_3NO (7.5 mg, 0.10 mmol). ^{13}C NMR spectra acquired at 193 K showed the formation of **4a** (6%), **4b** (62%), **4c** (16%) and of a novel species **4d** (16%) with carbonyl resonances at δ 206.0 (2), 199.4 (4), 195.5 (1), 190.08 (1), 188.9 (1) ppm. The addition of an excess of Me_3NO (ca. 6 mg, 0.08 mmol) gave mainly **4d**.

Preparation of $[\text{Re}_4\text{H}(\mu\text{-H})_2(\text{CO})_{17}]^-$ (2**) from $[\text{Re}_2(\text{CO})_9(\text{L})]$ and $[\text{Re}_2\text{H}_2(\mu\text{-H})(\text{CO})_8]^-$.** A THF solution of $[\text{Re}_2(\text{CO})_9(\text{L})]$, prepared from $[\text{Re}_2(\text{CO})_{10}]$ and Me_3NO , as above described (0.023 M, 0.90 mL, 0.020 mmol) was evaporated to dryness, the residue dissolved in CD_2Cl_2 , and the solution treated at 193 K with 1 equiv of $[\text{NEt}_4][\text{Re}_2\text{H}_2(\mu\text{-H})(\text{CO})_8]$ (14.5 mg, 0.020 mmol). ^1H -NMR monitoring showed the disappearance of the reagents in about 3 min at room temperature, to give mainly **2**. Unidentified hydridic resonances were observed at δ -6.13, -16.05, and -17.72 ppm (each one with an intensity approximately corresponding to one-half of the intensity of the signals of **2**).

Synthesis of $[\text{NEt}_4][\text{Re}_4(\mu\text{-H})(\text{CO})_{18}]$ ($[\text{NEt}_4]\mathbf{3}$). A sample of $[\text{NEt}_4][\text{Re}_2\text{H}(\text{CO})_9]$ (60 mg, 0.079 mmol) was added to a 0.020 M THF solution of $[\text{Re}_2(\text{CO})_9(\text{L})]$ (3.9 mL, 0.078 mmol) in CH_2Cl_2 , at 253 K. The solution was allowed to warm up to room temperature, concentrated, and then treated with *n*-hexane, to give a yellow precipitate of $[\text{NEt}_4][\text{Re}_4(\mu\text{-H})(\text{CO})_{18}]$ (66 mg, 0.048 mmol, isolated yield = 60%). Crystals suitable for X-ray analysis were obtained from $\text{CH}_2\text{Cl}_2/\textit{n}$ -hexane. Spectroscopic data of the anion **3**: IR (THF) $\nu(\text{CO})$ 2090 w, 2038 ms, 2009 sh, 1995 vs, 1971 s, 1950 ms, 1913 w, 1901 w; ^1H NMR (CD_2Cl_2 , 213 K) δ -17.42 ($\text{C}_3\text{D}_6\text{O}$, 193 K, δ -17.16 ppm); ^{13}C NMR (natural abundance, 193 K, CD_2Cl_2) δ 197.7 (6, A + C), 192.1 (1, D/E), 190.0 (1, E/D), 186.7 (1, B) ppm.

(21) Andrews, M. A.; Kirtley, S. W.; Kaesz, H. D. *Inorg. Chem.* **1977**, *16*, 1556.

(22) Beringhelli, T.; D'Alfonso, G.; Minoja, A. P.; Freni, M. *Gazz. Chim. Ital.* **1992**, *122*, 375.

(23) Chan, S. O.; Reeves, L. W. *J. Am. Chem. Soc.* **1973**, *95*, 673.

Preparation of ^{13}C -Enriched $[\text{NEt}_4][\text{Re}_4(\mu\text{-H})(\text{CO})_{18}]$. The reaction was performed as above, using ^{13}C -enriched $[\text{Re}_2(\text{CO})_9(\text{L})]$ (prepared from 40 mg, 0.061 mmol, of ^{13}C -enriched $[\text{Re}_2(\text{CO})_{10}]$ and ca. 6 mg, 0.078 mmol, of Me_3NO) and natural abundance $[\text{NEt}_4][\text{Re}_2\text{H}(\text{CO})_9]$ in CD_2Cl_2 (46 mg, 0.061 mmol). The ^{13}C NMR spectrum at 193 K showed the same carbonyl resonances observed in the natural abundance sample.

Reaction of $[\text{Re}_4\text{H}(\mu\text{-H})_2(\text{CO})_{17}]^-$ (2**) with CO.** A sample of $[\text{NEt}_4]\text{2}$ (16 mg, 0.012 mmol) was dissolved in 3 mL of THF under CO, and the solution was stirred at 253 K. IR monitoring showed the slow increase of the $\nu(\text{CO})$ bands of $[\text{Re}_2\text{H}(\text{CO})_9]^-$, $[\text{ReH}(\text{CO})_5]$, and $[\text{Re}_3\text{H}(\mu\text{-H})(\text{CO})_{13}]^-$. After 45 h, the solution was evaporated to dryness and the solvent, trapped at 193 K, showed the $\nu(\text{CO})$ band of $[\text{ReH}(\text{CO})_5]$. The ^1H NMR spectrum of the residue showed the resonances of $[\text{Re}_2\text{H}(\text{CO})_9]^-$, $[\text{Re}_3\text{H}(\mu\text{-H})(\text{CO})_{13}]^-$, and unreacted **2**. The reaction was also monitored by NMR. A sample of $[\text{NEt}_4]\text{2}$ (12 mg, 0.009 mmol), was dissolved in THF- d_8 under CO and stirred at 253 K for 120 h. ^{13}C and ^1H NMR spectra, acquired at 193 K, showed unreacted **2** (6%), $[\text{ReH}(\text{CO})_5]$ (60%), $[\text{Re}_2\text{H}(\text{CO})_9]^-$ (26%), and $[\text{Re}_3\text{H}(\mu\text{-H})(\text{CO})_{13}]^-$ (8%).

Reaction of $[\text{Re}_4(\mu\text{-H})(\text{CO})_{17}]^-$ (3**) with CO.** A sample of $[\text{NEt}_4]\text{3}$ (16 mg, 0.012 mmol) was dissolved in THF- d_8 in a Schlenk tube and the solution stirred under a CO atmosphere, at room temperature. NMR monitoring showed the slow disappearance of **3** (complete after 5 days) and the appearance of smaller resonances at δ -5.75 and -7.06 ppm (likely attributable to $[\text{ReH}(\text{CO})_5]$ and $[\text{Re}_2\text{H}(\text{CO})_9]^-$). The only other hydridic resonance observed at intermediate times was an unattributed one at δ -16.1 ppm (maximum intensity after 2 days, ca. 25% of that of **3**). The final reaction mixture was evaporated to dryness and washed with *n*-hexane, which extracted some $[\text{Re}_2(\text{CO})_{10}]$, recognized by IR.

X-ray Analysis of **2 and **3**. (a) Collection and Reduction of X-ray Data.** Suitable crystals of **2** and **3** were mounted in air on a glass fiber tip onto a goniometer head. Single-crystal X-ray diffraction data were collected on a Siemens SMART CCD area detector (at $T = 167$ K) for **2** and on an Enraf-Nonius CAD4 diffractometer at room temperature for **3**, using graphite-monochromatized Mo K α radiation ($\lambda = 0.71073$ Å). Unit cell parameters and an orientation matrix were obtained from least-squares refinement on 301 reflections measured in three different sets of 15 frames each in the range $0^\circ < \theta < 23^\circ$ for **2**, while for **3** the setting angles of 25 randomly distributed intense reflections with $10^\circ < \theta < 14^\circ$ were processed by least-squares fitting.

For **2** the intensity data were collected using the ω -scan technique within the limits $2.5^\circ < 2\theta < 53^\circ$ in the full sphere. The frame width was set to 0.3° , and the detector exposition for each frame was 20 s. The sample-detector distance was fixed at 5.5 cm. The first 100 frames were recollected at the end of data collection to have a monitoring of crystal decay, which was not observed; thus no time-decay correction was needed. The 2100 collected frames were then processed by SAINT software and an absorption correction was applied (SADABS) on the 28 900 ($R_\sigma = \sum[\sigma(F_o^2)]/\sum F_o^2 = 0.0243$) collected reflections, 4820 of which were unique, with $R_{\text{int}} = \sum|F_o^2 - F_{\text{mean}}^2|/\sum F_o^2 = 0.0395$.

For **3** the data collection was performed by the ω -scan method with variable scan speed (maximum time per reflection, 70 s) and variable scan range ($1.0^\circ + 0.35 \tan \theta$). The crystal stability under diffraction was checked by monitoring three standard reflections every 180 min. An empirical absorption correction was applied using ψ -scans of three suitable reflections having χ values close to 90° .²⁴ The measured intensities were corrected for Lorentz, polarization, background, and decay effects and reduced to F_o^2 . Selected crystal data are summarized in Table 4.

(b) Solution and Structure Refinement. The structures were solved by direct methods (SIR92²⁵) and difference Fourier

Table 4. Summary of Crystal Data and Structure Refinement Parameters for **2 and **3****

	2	3
formula	$\text{C}_{25}\text{H}_{23}\text{NO}_{17}\text{Re}_4$	$\text{C}_{26}\text{H}_{21}\text{NO}_{18}\text{Re}_4$
fw	1354.24	1380.24
cryst syst	orthorhombic	triclinic
space group	$Pbca$ (No. 61)	$P\bar{1}$ (No. 2)
<i>a</i> , Å	13.1036(4)	9.357(5)
<i>b</i> , Å	16.6438(8)	13.771(5)
<i>c</i> , Å	31.8384(8)	14.694(5)
α , deg		79.91(1)
β , deg		76.77(1)
γ , deg		79.93(1)
<i>V</i> , Å ³	6943.8(3)	1797(1)
<i>Z</i>	8	2
<i>F</i> (000)	4928	1256
<i>D</i> (calc), g cm ⁻³	2.591	2.551
temp, K	167(2)	293(2)
diffractometer	Siemens SMART	Enraf-Nonius CAD4
abs coeff, mm ⁻¹	13.972	13.505
cryst size, mm	0.33 × 0.27 × 0.18	0.23 × 0.20 × 0.15
scan method	ω	ω
2θ range, deg	2.5–53	6–50
index ranges, <i>h, k, l</i>	–15/15, –20/19, –38/38	–10/11, –15/16, 0/17
rfins colld, indep	37579, 4820	6286, 4125
cryst decay, %	0	11
abs correcn	SADABS	ψ -scan
min rel transm	0.47	0.72
data/restraints/parameters	4812/0/424	4117/0/442
goodness-of-fit on F_o^2 ^a	1.174	1.073
R_1, R_2 indexes ^b	0.0226, 0.0500	0.0278, 0.0622
max diff peak/hole, e Å ⁻³	0.861/–1.437	0.796/–1.094
weighting scheme, <i>a, b</i> ^c	0.0270, 5.246	0.0293, 9.015

^a GOF = $[\sum w(F_o^2 - F_c^2)^2/(n - p)]^{1/2}$ where *n* is the number of reflections and *p* is the number of refined parameters. ^b $R_1 = \sum|F_o| - |F_c|/\sum|F_o|$. $wR_2 = [\sum w(F_o^2 - F_c^2)^2/\sum wF_o^4]^{1/2}$. ^c $w = 1/[\sigma^2(F_o^2) + (aP)^2 + bP]$ where $P = (F_o^2 + 2F_c^2)/3$.

methods; they were refined by full-matrix least squares against F_o^2 using reflections with $F_o^2 \geq 3\sigma(F_o^2)$ and the program SHELXL93.²⁶ Scattering factors for neutral atoms and anomalous dispersion corrections were taken from ref.²⁷ Anisotropic displacement parameters were assigned to all non-hydrogen atoms. The positions of the hydride ligands were evidenced by a difference Fourier map and were in agreement with the local stereogeometry around the metal centers (lengthening of the M–M interactions and widening of the M–M'–L angles adjacent to the $\mu\text{-H}$ ligands, and an apparent hole in the coordination sphere for the terminal hydride). More accurate positions of the hydrides were eventually calculated by means of the program HYDEX²⁸ with $d_{\text{M-H}} = 1.85$ Å for both terminal and bridging hydrides. Hydrogen atoms of the tetraethylammonium cations were placed in idealized positions with an isotropic displacement parameter 1.5 times that of the pertinent carbon atom. The hydrogens were introduced in the final stages of structure factor calculations but not refined.

The final conventional agreement indexes are listed in Table 4.

Supporting Information Available: Tables containing final atomic coordinates, anisotropic displacement parameters, a full listing of bond distances and angles, and least-squares planes (10 pages). Ordering information is given on any current masthead page.

OM970332L

(25) Altomare, A.; Cascarano, G.; Giacovazzo, C.; Guagliardi, A.; Burla, M. C.; Polidori, G.; Camalli, M. *J. Appl. Crystallogr.* **1994**, *27*, 435.

(26) Sheldrick, G. M. *SHELXL-93: program for structure refinement*; University of Goettingen: Goettingen, 1994.

(27) *International Tables for Crystallography*; Kluwer: Dordrecht, 1992; Vol. C, Tables 4.2.6.8 and 6.1.1.4.

(28) Orpen, A. G. *J. Chem. Soc., Dalton Trans.* **1980**, 2509.

(24) North, A. C. T.; Phillips, D. C.; Mathews, F. S. *Acta Crystallogr., Sect. A* **1968**, *24*, 351.